

Selective Complexation and Separation of Uranium(VI) from Thorium(IV) with New Tetradentate N,O-Hybrid Diamide Ligands: Synthesis, Extraction, Spectroscopy, and Crystallographic Studies

Ying Wang, Yuxiang Yang, Yijie Wu, Jin Li, Bowen Hu, Yimin Cai,* Lihua Yuan, and Wen Feng*



Cite This: *Inorg. Chem.* 2023, 62, 4922–4933



Read Online

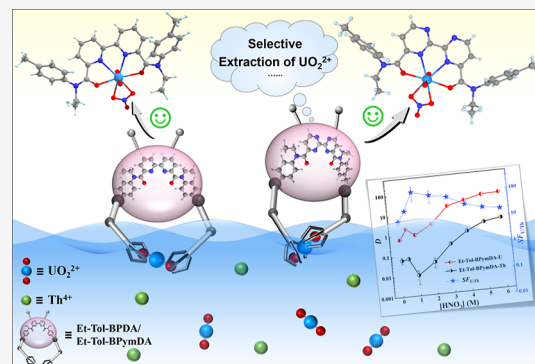
ACCESS |

Metrics & More

Article Recommendations

Supporting Information

ABSTRACT: An unmet challenge in the thorium-uranium fuel cycle is the efficient separation of uranium from thorium. Herein, two new tetradentate N,O-hybrid ligands, *N,N'*-diethyl-*N,N'*-di-*p*-tolyl-2,2'-bipyridine-6,6'-dicarboxamide (Et-Tol-BPDA) and *N,N'*-diethyl-*N,N'*-di-*p*-tolyl-2,2'-bipyrimidine-4,4'-dicarboxamide (Et-Tol-BPymDA), comprising a bipyridine or bipyrimidine core and amide moieties were designed and synthesized for selectively complexing and separating U(VI) from Th(IV). The high U(VI)/Th(IV) extraction selectivity was achieved by Et-Tol-BPDA ($SF_{U/Th} = 33$ at 3 M HNO₃) and Et-Tol-BPymDA ($SF_{U/Th} = 73$ at 3 M HNO₃) in nitric acid solutions. The extraction process for U(VI) or Th(IV) with these two ligands primarily proceeded through the solvation mechanism, as evidenced by slope analyses. Thermodynamic studies for the extraction of U(VI) and Th(IV) revealed a spontaneous process. Results from UV-vis spectroscopic titration and slope analyses demonstrated that U(VI) and Th(IV) each form a 1:1 complex with the two ligands both in the monophasic organic solution and the biphasic extraction system. The stability constants of the 1:1 complexes of Et-Tol-BPDA or Et-Tol-BPymDA with U(VI) were found to be larger than those with Th(IV), which coincide well with the high U(VI)/Th(IV) extraction selectivity. The solid-state structures of Et-Tol-BPDA, Et-Tol-BPymDA, and 1:1 complexes of the two ligands with U(VI) or Th(IV) were analyzed by X-ray diffraction technique. The results from this work implicate the potential of bipyridine- and bipyrimidine-derived diamide ligands for uranium/thorium separation.



INTRODUCTION

Facing the ever-growing low-carbon energy demand and ensuring energy security, thorium-based molten salt reactors (TMSRs) for the Gen-IV nuclear reactor system have attracted escalating attention in recent years.^{1,2} Compared to the well-known uranium-plutonium fuel cycle, the thorium-uranium fuel cycle offers several potential merits, such as high actinide burnup, less long-lived minor actinide production, intrinsic nuclear proliferation resistance, and so forth.^{3,4} Thorium in the earth's crust is 3–4 times more abundant than uranium (the worldwide thorium resources amount to 6.35–6.37 million tonnes⁵) and naturally exists in a monoisotopic form of ²³²Th,⁶ and thus the use of thorium could greatly reduce energy-intensive enrichment activities and mining operations. As the counterpart of ²³⁹Pu in the uranium-plutonium fuel cycle, the fissile nucleus ²³³U could be produced via neutron capture on the fertile material ²³²Th in breeder reactors^{6,7} and then separated and recovered during the reprocessing of irradiated thorium for ultimate use as a fuel. To this end, sequestering uranium from irradiated thorium is critically important in terms of both ensuring the successful operation of the thorium fuel cycle and improving the sustainability and economics of the nuclear fuel cycle. However, the efficient and selective

separation of uranium remains a formidable task because of the similar physicochemical properties as well as the invariable oxidation state of thorium.⁸

To address this issue, extensive endeavors have been devoted to uranium/thorium separation, and different technologies have been developed, such as solvent extraction,⁹ adsorption,¹⁰ precipitation,¹¹ ion exchange,¹² etc. Of them, solvent extraction plays a dominating role in the nuclear industry, benefiting from its facile process and high sample throughput.^{13,14} The thorium-uranium extraction (Thorex) process, based on the solvent extraction technique with tri-*n*-butyl-phosphate (TBP, Figure 1) in a hydrocarbon diluent, represents one of the most promising methods for separating uranium and thorium from fission products and from each other.^{8,15} However, it is well known that TBP suffers from drawbacks of high water solubility and formation of the third

Received: December 14, 2022

Published: March 15, 2023



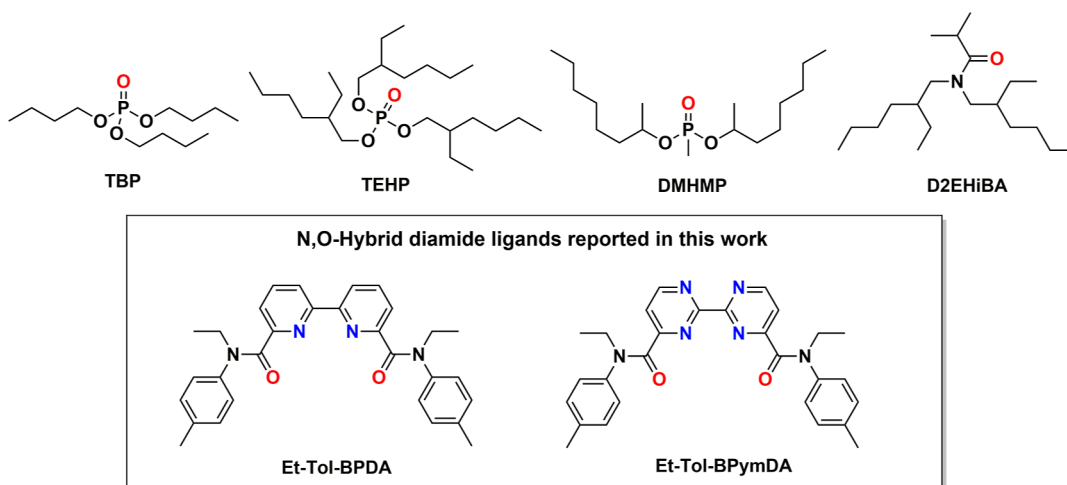


Figure 1. Molecular structures of extractants for U(VI)/Th(IV) separation.

phase.¹⁶ Elongation of the alkyl chain and introduction of branching on the alkyl chain endow the organophosphorus compounds, e.g., tris-2-ethyl-hexyl phosphate (TEHP)^{17,18} and di(1-methyl-heptyl)methyl phosphonate (DMHMP)^{7,19} with lower water solubility and a more steric effect upon Th(IV) complexation relative to TBP. As a result, TEHP and DMHMP displayed superior selectivity for U(VI) over Th(IV) compared to that of TBP in nitric acid solutions (1–5 M), and a reduced tendency to form the third phase.^{18,19} However, the non-incinerable nature of these organophosphorus extractants leads to the production of a lot of secondary radioactive waste, which severely hamper their practical applications. The U(VI)/Th(IV) separation at high acidity was also tried by employing branched-chain *N,N*-dialkyl amides that exhibit higher affinity for hexavalent actinides than tetravalent ones.²⁰ For instance, *N,N*-di(2-ethylhexyl)isobutyramide (D2EHIBA) could extract trace amounts of U(VI) with a high separation factor [the ratio between the distribution ratio of U(VI) and Th(IV)] of 2975, but the distribution ratio of U(VI) is rather low ($D_U = 1.2$).²¹ Therefore, it is still highly desirable for new ligands to have high extraction ability and selectivity for U(VI) over Th(IV).

The past decade has witnessed a flourishing development of actinide/lanthanide complexation and separation by employing N,O-hybrid ligands based on rigid N-heterocyclic skeletons.^{22–31} Shi et al. reported a tetradentate N,O-hybrid ligand, *N,N'*-diethyl-*N,N'*-ditolyl-2,9-diamide-1,10-phenanthroline (Et-Tol-DAPhen), with well-preorganized amide oxygen and nitrogen atoms, which exhibits good extraction ability and selectivity toward actinides over lanthanides.²² More recently, Zabierowski et al.³⁰ reported that 2,2'-bipyrimidine-4,4'-dicarboxylic acid could bind to lanthanides to form stable complexes, in which the pyrimidine nitrogen atoms and carboxylic oxygen atoms involved in coordination on the same molecule always lie approximately in the same plane. It thus can be envisaged that this kind of N,O-hybrid ligand would show preferential coordination toward U(VI) over Th(IV) as the coordination of uranyl ions merely occurs in the equatorial plane,^{32–35} while thorium ions always exhibit spherical coordination with a wide range of coordination numbers (5–12).^{36,37} Until now, employing N,O-hybrid ligands for U(VI)/Th(IV) separation still remains a rarely explored territory.²² In this backdrop, we report herein two new tetradentate N,O-hybrid ligands, *N,N'*-diethyl-*N,N'*-di-*p*-tolyl-2,2'-bipyridine-6,6'-dicarboxamide (Et-Tol-BPDA, Figure 1)

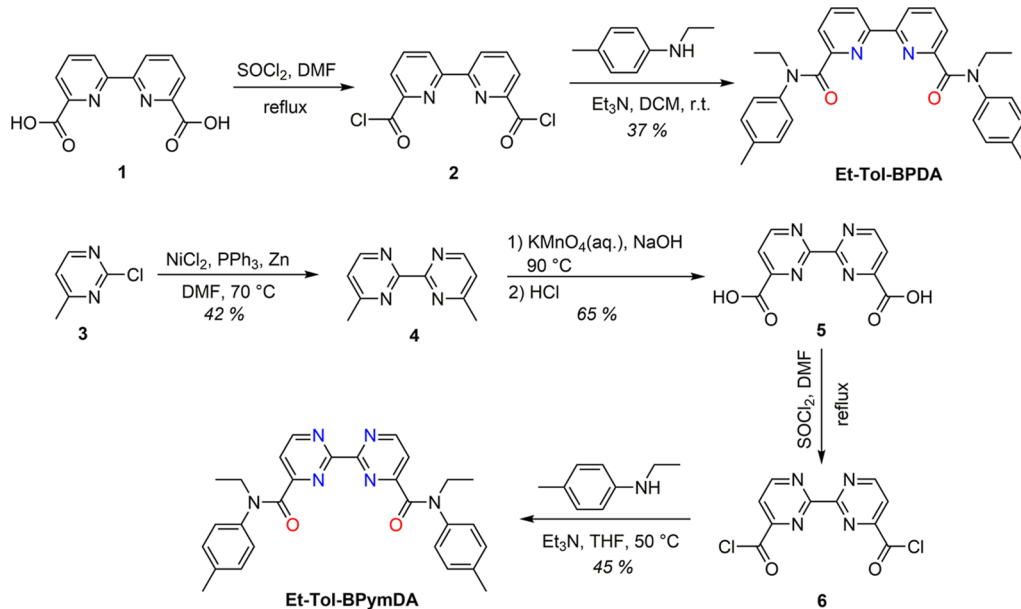
and *N,N'*-diethyl-*N,N'*-di-*p*-tolyl-2,2'-bipyrimidine-4,4'-dicarboxamide (Et-Tol-BPymDA), furnished with a bipyridine or bipyrimidine skeleton and amide groups for the selective extraction of U(VI) over Th(IV). The extraction performance, including the effects of contact time, nitric acid concentration, ligand concentration, and temperature, as well as the extraction mechanism of the two ligands were assessed by systematic solvent extraction experiments. In addition, UV-vis titration and single-crystal X-ray diffraction experiments were performed to probe the complexation behaviors and the coordination mode between the two ligands and U(VI) or Th(IV).

EXPERIMENTAL SECTION

Chemicals and Methods. Chemical reagents used in synthetic experiments and solvent extraction experiments, including 2,2'-bipyridine-4,4'-dicarboxylic acid, 2-chloro-4-methylpyrimidine, *N*-ethyl-*p*-toluidine, 1-butyl-3-methylimidazolium bis((trifluoromethyl)sulfonyl)amide ($C_4\text{mimNTf}_2$), lithium bis(trifluoromethanesulfonyl)-imide (LiNTf_2), 1-butyl-3-methylimidazolium chloride ($C_4\text{mimCl}$), $\text{UO}_2(\text{NO}_3)_2 \cdot 6\text{H}_2\text{O}$, $\text{Th}(\text{NO}_3)_4$, and other inorganic/organic reagents of their purest forms, were all obtained commercially and used without further purification. ^1H NMR and ^{13}C NMR spectra were collected on a Bruker AVANCE III HD-400 MHz at 298 K. Mass spectra were recorded on a high-resolution liquid chromatograph coupled with a mass spectrometer.

Synthesis. The specific synthetic procedures of Et-Tol-BPDA, 4,4'-dimethyl-2,2'-bipyrimidine,³⁰ and 2,2'-pyrimidine-4,4'-dicarboxylic acid³⁸ are described in the Supporting Information.

Et-Tol-BPymDA. 2,2'-Bipyrimidine-4,4'-dicarboxylic acid (1.60 g, 6.50 mmol) was refluxed with thionyl chloride (15 mL) and a drop of *N,N*-dimethylformamide in an argon atmosphere for 3 h. The excess thionyl chloride was removed under reduced pressure, and the resulting red brown solid was dissolved in dry tetrahydrofuran (100 mL). Subsequently, *N*-ethyl-*p*-toluidine (3.52 g, 26 mmol) and triethylamine were added slowly into this solution at room temperature. The resulting solution was stirred overnight at 50 °C, followed by removing the solvent under reduced pressure. The crude product was dissolved in dichloromethane (100 mL) and washed with deionized water (100 mL × 3), after which the organic phase was collected and dried over anhydrous Na_2SO_4 . After purification by flash column chromatography (dichloromethane/methanol, 100:1, v/v), Et-Tol-BPymDA was obtained as a slightly yellow solid (1.4 g, 45%). ^1H NMR (400 MHz, CDCl_3): δ 8.79 (d, $J = 5.0$ Hz, 2H), 7.22 (d, $J = 5.0$ Hz, 2H), 7.01 (d, $J = 8.2$ Hz, 4H), 6.95 (d, $J = 8.1$ Hz, 4H), 3.98 (q, 4H), 2.20 (s, 6H), 1.23 (t, $J = 7.2$ Hz, 6H). ^{13}C NMR (100 MHz, CDCl_3): δ 166.00, 163.01, 161.49, 158.07, 138.23, 137.64, 129.89,

Scheme 1. Synthetic Routes of Et-Tol-BPDA and Et-Tol-BPymDA

128.24, 119.58, 44.63, 20.93, 12.67. ESI-MS (*m/z*): calcd for [M + H]⁺ 481.2347; found [M + H]⁺ 481.2364.

The ¹H NMR, ¹³C NMR, and electrospray ionization-high-resolution mass spectrometry (ESI-HRMS) spectra of Et-Tol-BPDA and Et-Tol-BPymDA are depicted in the Supporting Information (Figures S1–S6).

Solvent Extraction Experiments. The aqueous phase consists of the solution of U(VI) (50 mg/L) or Th(IV) (50 mg/L) in nitric acid with different concentrations (0.1–6 M). The organic phase was prepared by dissolving certain weights of ligand in C₄mimNTf₂ or other traditional organic diluents. In a typical solvent extraction experiment, equal volumes of the organic and aqueous phases (0.5 mL) were added into a stoppered tube and vigorously shaken for 6 h at 298 ± 1 K. After centrifugation and phase separation, 0.2 mL of the aqueous phase was taken for inductively coupled plasma-optical emission spectrometry (ICP-OES; PerkinElmer ICP Optima 8000) analysis. All the solvent extraction experiments were carried out in duplicate with acceptable errors. The distribution ratio (*D*) was calculated as the ratio of the metal ion concentration in the organic phase to that in the aqueous phase (*D* = [M]_{org}/[M]_{aq}, where [M]_{org} and [M]_{aq} represent the concentration of metal ions in the organic and aqueous phases, respectively). The separation factor (*SF*) was obtained as the ratio between the *D* values of two metal ions (*SF*_{U/Th} = *D*_U/*D*_{Th}).

For nitric acid extraction experiments, equal volumes of nitric acid solution and C₄mimNTf₂, with or without ligand, were contacted and shaken for 6 h. The initial and equilibrium nitric acid concentrations of the aqueous phase were determined by volumetric titration using 0.1 M NaOH standard solution and the phenolphthalein indicator.

For the stripping of U(VI), the metal ion-loaded organic phase was contacted with an equal volume of stripping agents in a stoppered glass tube. After shaking for 2 h and centrifugation, the metal ion concentration of the aqueous phase was determined by ICP-OES.

UV-Vis Spectroscopic Titration. All UV-vis spectroscopic experiments were conducted on a SHIMADZU UV-2450 spectrophotometer in acetonitrile at 298 ± 1 K. The Job plot experiments were carried out with the concentration of [L] + [M] being fixed at 50 μM. In a typical titration experiment, the ligand solution (3 mL, 20 μM) was titrated with UO₂(NO₃)₂ or Th(NO₃)₄ solution (600 μM, 10 μL for each titration) and then stirred vigorously for at least 5 min to achieve complexation equilibrium. Tetraethylammonium nitrate (Et₄NNO₃, 2.5 mM) was added into titration solutions to fix the ionic strength (*I*). Absorption spectra were collected in the wavelength range of 250–400 nm. The stability constants of the

L–Mⁿ⁺ complexes were determined by a global fitting analysis to a 1:1 binding model using the website (<http://supramolecular.org/>).³⁹

Preparation of Single-Crystal Complexes and X-ray Diffraction Measurements. **Et-Tol-BPDA (1).** The ligand Et-Tol-BPymDA (10 mg, 0.021 mmol) was dissolved in 0.5 mL methanol. After slow evaporation at room temperature for a week, colorless crystals of Et-Tol-BPDA were obtained.

Et-Tol-BPymDA (2). The ligand Et-Tol-BPymDA (12 mg, 0.025 mmol) was dissolved in 1 mL of methanol, and 0.5 mL of deionized water was added. After slow evaporation at room temperature for about five days, colorless crystals of Et-Tol-BPymDA were obtained.

[UO₂(Et-Tol-BPDA)(NO₃)₂]·UO₂(NO₃)₃·NO₃ (3). A solution of Et-Tol-BPDA (12 mg, 0.025 mmol) in 2 mL of dichloromethane was mixed with a solution of UO₂(NO₃)₂·6H₂O (13 mg, 0.025 mmol) in 1 mL of ethanol. After slow evaporation at room temperature for 3 days, yellow block-like crystals were obtained.

UO₂(Et-Tol-BPymDA)(NO₃)₂·UO₂(NO₃)₃ (4). A solution of Et-Tol-BPymDA (12 mg, 0.025 mmol) in 2 mL of dichloromethane was mixed with a solution of UO₂(NO₃)₂·6H₂O (13 mg, 0.025 mmol) in 2 mL of ethanol. After stirring for 3 h, the resulting solution was left to evaporate slowly at room temperature. Yellow rod-shaped crystals were obtained over 2 days.

[Th(Et-Tol-BPDA)(NO₃)₄]₂·(CH₂Cl₂)₃ (5). A solution of Et-Tol-BPDA (12 mg, 0.025 mmol) in 1 mL of dichloromethane was added into a solution of Th(NO₃)₄ (12 mg, 0.025 mmol) in 1 mL of acetonitrile. After vapor diffusion of diethyl ether to this resulting solution at room temperature for 2 days, pale-yellow block-like crystals were obtained.

Th(Et-Tol-BPymDA)(NO₃)₄·(CH₃CN)₂ (6). The ligand Et-Tol-BPymDA (12 mg, 0.025 mmol) was dissolved in 1 mL of acetonitrile. To this solution was added a solution of Th(NO₃)₄ (12 mg, 0.025 mmol) in 0.5 mL of deionized water. After slow evaporation at room temperature overnight, light-yellow flaky crystals were obtained.

The single-crystal X-ray diffraction measurements were conducted on a Bruker APEX-II CCD diffractometer equipped with MoKα radiation ($\lambda = 0.71073$). Crystal data and structure refinement parameters are provided in Tables S7 and S8.

RESULTS AND DISCUSSION

Synthesis and Characterization. The new ligand Et-Tol-BPDA was synthesized starting from the acyl chlorination of commercially available 2,2'-bipyridine-4,4'-dicarboxylic acid, followed by reacting with N-ethyl-p-toluidine to afford the

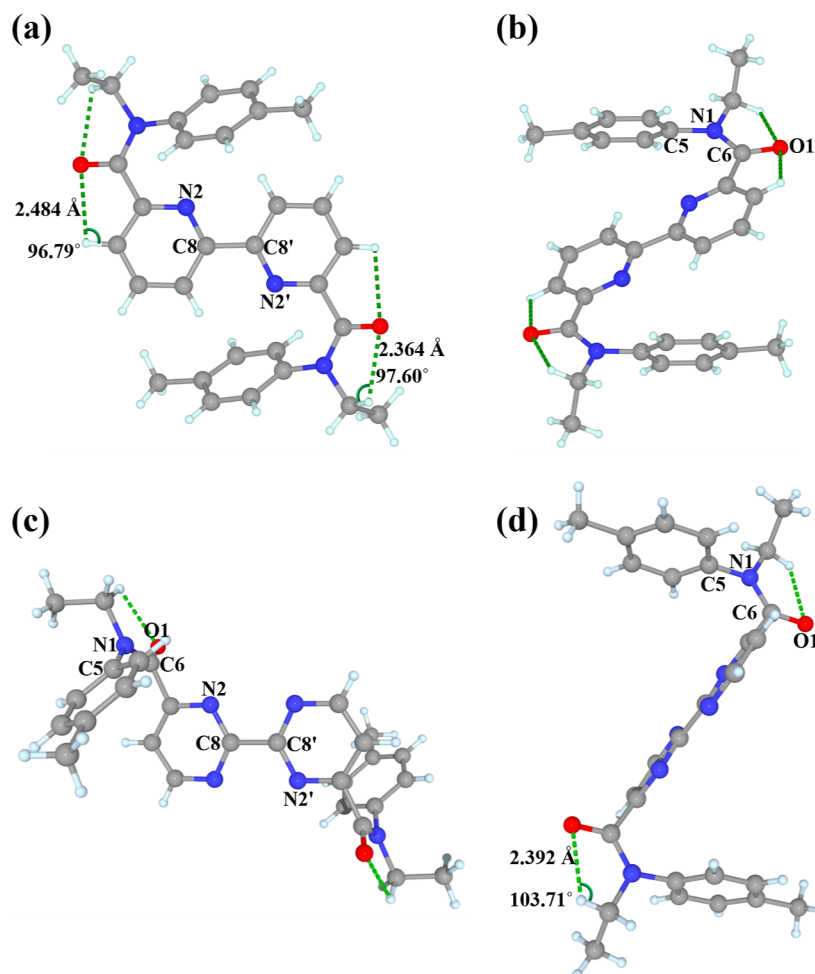


Figure 2. Crystal structures of Et-Tol-BPDA and Et-Tol-BPymDA. (a) Top view and (b) side view of Et-Tol-BPDA. (c) Top view and (d) side view of Et-Tol-BPymDA. Gray, blue, red, and light turquoise colors denote C, N, O, and H atoms, respectively. The green dashed lines represent the intramolecular hydrogen bonds.

desired product in a yield of 37% (**Scheme 1**). Et-Tol-BPymDA was synthesized in four steps (**Scheme 1**). First, 2-chloro-4-methyl pyrimidine (**3**) was converted to 4,4'-dimethyl-2,2'-bipyrimidine (**4**) by the Tiecco coupling reaction, according to the reported literature.³⁰ Compound **4** was then oxidized with potassium permanganate at 90 °C, followed by treatment with hydrochloric acid to generate 2,2'-bipyrimidine-4,4'-dicarboxylic acid (**5**) in a yield of 65%.³⁸ After refluxing dicarboxylic acid **5** with thionyl chloride in the presence of a catalytic amount of *N,N*-dimethylformamide for 3 h, the remaining diacyl chloride **6** was obtained by removing the excess thionyl chloride and solvent and then reacted with *N*-ethyl-*p*-toluidine and triethylamine in tetrahydrofuran to provide Et-Tol-BPymDA in a reasonable yield of 45%.

The solid-state structures of the ligands Et-Tol-BPDA and Et-Tol-BPymDA were characterized by single-crystal X-ray diffraction. Their bond distance and bond angle data are summarized in **Tables S9–S12**. The ligands Et-Tol-BPDA and Et-Tol-BPymDA are crystallized in the monoclinic space group *P*2₁/c and the triclinic space group *P*1, respectively. The crystal structures of Et-Tol-BPDA and Et-Tol-BPymDA possess a center of symmetry at the middle of the C8–C8' bond of the bipyridine or bipirimidine moiety (**Figure 2a,c**). Moreover, both the bipyridine and bipirimidine skeletons take a planar conformation with the torsion angle N2–C8–C8'-N2' of

180.00°. As illustrated in **Figure 2b**, each of the two tolyl groups on Et-Tol-BPDA is *trans* in relation to the oxygen atom of amide groups, and the torsion angle O1–C6–N1–C5 is about 171.73°. The similar *trans* conformation of aromatic groups of *N*-ethyl anilide with respect to amide oxygens was also observed in the solid-state structure of Et-Tol-BPymDA with the torsion angle O1–C6–N1–C5 of 178.41° (**Figure 2d**), as well as other reported N,O-hybrid diamides, such as *N,N'*-diethyl-*N,N'*-bis(2-fluorophenyl)-2,2'-bipyridine-6,6'-dicarboxamide⁴⁰ and *N,N'*-diethyl-*N,N'*-diphenyl-2,2'-bipyridine-6,6'-dicarboxamide.⁴¹ In addition, multiple intramolecular C–H···O hydrogen bonds and intermolecular C–H···N hydrogen bonds (**Figure S7**) are observed to stabilize the trans configuration of these two diamide molecules in the solid state.

Solvent Extraction Properties. Room-temperature ionic liquids (RTILs) as an organic molten salts have shown considerable potential in use as the diluent in solvent extraction experiments, owing to their advantages of good stability, negligible volatility, and excellent solubility for the organic ligands and extracted complexes.^{42–44} Before performing systematic solvent extraction experiments, different common diluents, including *n*-octanol, dichloromethane, 1,2-dichloroethane, chloroform, 3-nitrobenzotrifluoride, and the RTIL, C₄mimNTf₂ (**Figure S8**) were tested at 3 M HNO₃

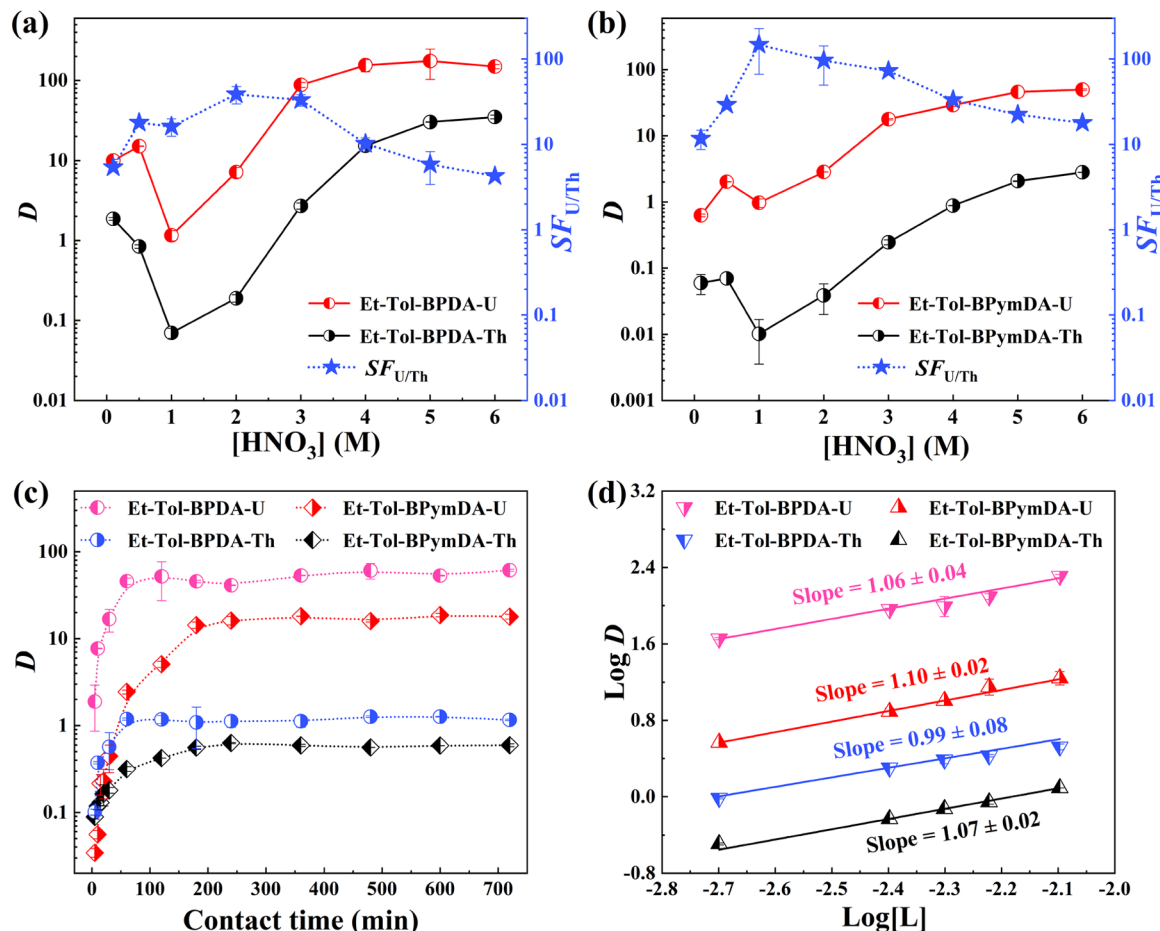


Figure 3. Distribution ratios of U(VI) and Th(IV) with Et-Tol-BPDA or Et-Tol-BPymDA as functions of (a) HNO_3 concentration (Et-Tol-BPDA), (b) HNO_3 concentration (Et-Tol-BPymDA), (c) contact time, and (d) ligand concentration. Unless otherwise specified, the organic phase was 5 mM ligand in $C_4mimNTf_2$, and the aqueous phase was 50 mg/L U(VI) or Th(IV) in 3 M HNO_3 .

(Tables S1 and S2). The results indicated that both Et-Tol-BPDA and Et-Tol-BPymDA dissolved in $C_4mimNTf_2$ exhibit the best selectivity for U(VI) over Th(IV). Therefore, $C_4mimNTf_2$ was selected as the diluent in this work.

Influence of Nitric Acid Concentration. Both the ligands and the ionic liquid may extract nitric acid from aqueous phase into organic phase. Therefore, the extraction of nitric acid by $C_4mimNTf_2$ with or without 5 mM ligands was first studied at acidities ranging from 0.1 to 6 M HNO_3 (Figure S9). It was found that in all the cases, the extraction of HNO_3 is negligible (<5%) at 0.1–4 M HNO_3 . The elevation of initial acid concentration leads to higher acid extraction, but the extraction percentages of nitric acid are invariably less than 10% in all the acidity tested. A similar trend for nitric acid extraction by $C_4mimNTf_2$ systems was also found by Billard et al.⁴⁵

The acidity of aqueous phase is one of the most significant factors that affect metal ion complexation and extraction. The extraction experiments of U(VI) and Th(IV) with Et-Tol-BPDA and Et-Tol-BPymDA were conducted at different HNO_3 concentrations from 0.1 to 6 M. For Et-Tol-BPDA, the increase of acidity from 0.1 to 1 M HNO_3 causes an initial drop of D_U and D_{Th} values (Figure 3a) and then leads to a remarkable increase in distribution ratios for both U(VI) and Th(IV) at higher acidity (>1 M HNO_3). The decrease of the D values at low acidity is ascribed to the protonation of the ligands, thus diminishing the complexation ability of Et-Tol-

BPDA, while the rise of extraction at high acidity is probably due to the increased concentration of the nitrate anion in the aqueous phase. The nitrate anions can be coextracted into the organic phase for charge balance, as proved by slope analyses (vide post). At all the tested acidities, the extraction of U(VI) is always much higher than that of Th(IV), with the $SF_{U/Th}$ values reaching up to 39 (Table S3). Similar extraction behaviors for U(VI) and Th(IV) at 0.1–6 M HNO_3 were also found with Et-Tol-BPymDA (Figure 3b). Although the distribution ratios are lower than those of Et-Tol-BPDA, the U(VI)/Th(IV) separation with Et-Tol-BPymDA provides better $SF_{U/Th}$ values of 147 at 1 M HNO_3 and 73 at 3 M HNO_3 (Tables S4 and S5).

Influence of Contact Time. Extraction kinetics for both U(VI) and Th(IV) was investigated at different contact times (0–720 min). As shown in Figure 3c, the distribution ratios of U(VI) and Th(IV) for Et-Tol-BPDA and Et-Tol-BPymDA at 3 M HNO_3 increase prominently with increasing contact time and show plateaus at 120 and 180 min, respectively, revealing the establishment of extraction equilibrium. The relatively slow kinetics was also widely observed in other extraction systems based on ionic liquids,^{46,47} which is mainly attributable to the high viscosity of ionic liquids, thereby suppressing the mass transfer rates of species and eventually slowing the extraction kinetics.⁴³ To ensure the extraction equilibrium, the contact time for the following solvent extraction experiments was fixed at 360 min. In addition, Et-Tol-BPDA clearly exhibits a higher

D value toward U(VI) and Th(IV) relative to Et-Tol-BPymDA. The lower extractability of Et-Tol-BPymDA can be explained by the electron-withdrawing effect of the two additional nitrogen atoms with respect to Et-Tol-BPDA, thus leading to lower extraction for metal ions. This is consistent with the lower natural charges of the two nitrogen atoms near the amide groups in Et-Tol-BPDA (-0.493) than those in Et-Tol-BPymDA (-0.476) from theoretical calculations (Figure S10).

Influence of Ligand Concentration. Figure 3d shows the extraction results of U(VI) and Th(IV) from 3 M HNO₃ to organic phases containing varying concentrations of Et-Tol-BPDA or Et-Tol-BPymDA. As the extractant concentration increases from 2 to 8 mM, the *D* values of both U(VI) and Th(IV) increase noticeably. The increase in *D* values upon increasing the ligand concentration indicates that the complexation between the ligands and metal ions is the driving force for the extraction processes. In addition, both the slope values of logD_U and logD_{Th} versus log[L] are close to 1, pointing to the formation of 1:1 complexes between ligands and U(VI) or Th(IV) during the extraction process (See eqs S1–S8 in Supporting Information for the detailed derivation).

Stripping Study. From the point of view of recovering metal ions and reusing the organic phase, an important aspect for evaluating an extraction system is the stripping efficiency. Therefore, the back extraction of U(VI) from the loaded organic phase was examined. As listed in Table 1, deionized

Table 1. Stripping of U(VI) from the Loaded Organic Phase^a

stages	Et-Tol-BPDA			Et-Tol-BPymDA	
	deionized water (%)	0.01 M HNO ₃ (%)	0.05 M EDTA-2Na + 1 M guanidine carbonate (%)	deionized water (%)	0.01 M HNO ₃ (%)
I	2.7	5.9	97.1	53.3	51.1
II	16.2	14.3	98.5	96.6	94.9
III	22.6	19.3	99.8	96.9	99.8

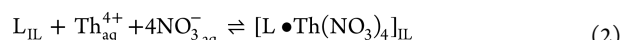
^aThe organic phase containing 5 mM ligand.

water or 0.01 M HNO₃ could efficiently strip U(VI) from the Et-Tol-BPymDA/C₄mimNTf₂ system, and almost quantitative stripping of U(VI) was achieved after three stages. For the Et-Tol-BPDA/C₄mimNTf₂ system, deionized water or 0.01 M HNO₃ failed to back extract U(VI), while a solution of 0.05 M EDTA-2Na and 1 M guanidine carbonate is able to almost completely strip U(VI) after three stages.

Extraction Mechanism Elucidation. To ascertain the extraction mechanism in the Et-Tol-BPDA/C₄mimNTf₂ and Et-Tol-BPymDA/C₄mimNTf₂ system, variations in the distribution ratio of U(VI) and Th(IV) as a function of C₄mim⁺ or NTf₂⁻ concentration in the aqueous phase were tested at 3 M HNO₃. As shown in Figure 4a–d, the D_U and D_{Th} values of Et-Tol-BPDA and Et-Tol-BPymDA changed marginally with increasing C₄mim⁺ or NTf₂⁻ concentrations, but the absolute values of slope from the linear plots of logD versus log[C₄mim⁺] and log[NTf₂⁻] are far less than 1, suggesting that neither C₄mim⁺ nor NTf₂⁻ is involved in the extraction mechanism and that the extraction of U(VI) and Th(IV) with Et-Tol-BPDA/C₄mimNTf₂ and Et-Tol-BPymDA/C₄mimNTf₂ systems follows the solvation mechanism at 3 M HNO₃. Therefore, the charge transfer between the two phases during

metal ion extraction is principally balanced by the coextraction of nitrate anions into the organic phase rather than the cation exchange of C₄mim⁺.

This is further confirmed by the following extraction experiments with varying nitrate concentrations in the aqueous phase. Figure 4e,f shows that both the D_U and D_{Th} values of Et-Tol-BPDA and Et-Tol-BPymDA increase continuously with increasing initial nitrate concentrations in the aqueous phase. Slopes of 1.82 ± 0.24 and 2.21 ± 0.11 were obtained from the plot of logD_U versus log[NO₃⁻], suggesting that two nitrate anions are extracted into the organic phase to balance the two positive charges of each uranyl ion. For the extraction of Th(IV), the slope of logD_{Th} versus log[NO₃⁻] was calculated to be 3.80 ± 0.22 and 3.81 ± 0.22 for Et-Tol-BPDA and Et-Tol-BPymDA, respectively, indicative of the participation of four nitrate anions in the extraction of each thorium ion. Based on the ligand/metal stoichiometry of 1:1 for the two ligands derived by the aforementioned slope analyses (Figure 3d), the extraction equilibrium for U(VI) and Th(IV) can be deduced as follows



where L represents the ligand. The subscripts “IL” and “aq” indicate that the species is in the IL phase and the aqueous phase, respectively.

Extraction Thermodynamics. For a better understanding of the extraction behavior of the two ligands, thermodynamic parameters were determined by implementing solvent extraction experiments at various temperatures from 293.15 to 313.15 K. As illustrated in Figure S11a, the D_U and D_{Th} values of Et-Tol-BPDA rise continuously with increasing temperature, indicative of the endothermic nature of the Et-Tol-BPDA/C₄mimNTf₂ system for the extraction of U(VI) and Th(IV). On the contrary, raising temperature reduced the D_U and D_{Th} values of Et-Tol-BPymDA (Figure S11b), signaling the exothermic nature of the extraction process. The apparent extraction equilibrium constant (K_{ex}) for the two ligands at different temperatures was calculated. The plots of 1/T against logK_{ex} are shown in Figure 5. Besides, the enthalpy change (ΔH), the entropy change (ΔS), and the change in Gibbs free energy (ΔG) during the extraction process were determined through the Van't Hoff (eq 3) and thermodynamic (eq 4) equations shown below

$$\log K_{ex} = -\Delta H/2.303RT + \Delta S/2.303R \quad (3)$$

$$\Delta G = \Delta H - T\Delta S = -2.303RT \log K_{ex} \quad (4)$$

where R stands for the universal gas constant of $8.314 \text{ J mol}^{-1} \text{ K}^{-1}$. As listed in Table S6, for Et-Tol-BPDA, positive changes in entropy mean that the extraction of metal ions with Et-Tol-BPDA enhances the degree of freedom of the extraction system. Negative ΔG values at 298.15 K suggest that the extraction of U(VI) and Th(IV) in the Et-Tol-BPDA/C₄mimNTf₂ system occurs spontaneously. More negative ΔG values for U(VI) ($-13.38 \pm 0.08 \text{ kJ mol}^{-1}$) compared to that of Th(IV) ($-0.61 \pm 0.21 \text{ kJ mol}^{-1}$) reveal that the extraction of uranyl is more favorable than thorium. In the case of Et-Tol-BPymDA, negative ΔG values indicate that the extraction process of U(VI) and Th(IV) with Et-Tol-BPymDA at 298.15 K is spontaneous in nature, and negative values of ΔH and ΔS

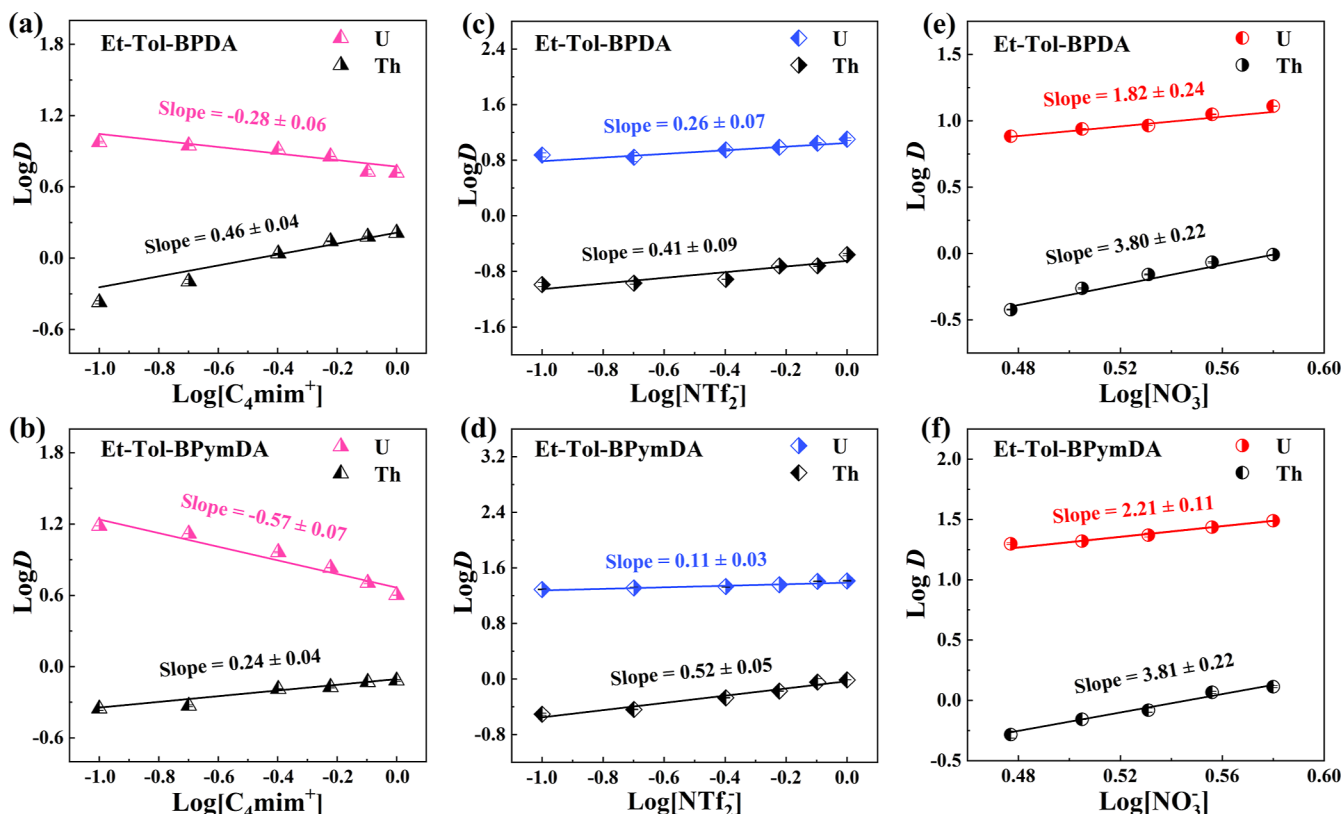


Figure 4. Distribution ratios of U(VI) and Th(IV) with ligands as functions of (a) C_4mim^+ concentration (Et-Tol-BPDA), (b) C_4mim^+ concentration (Et-Tol-BPymDA) (aqueous phase: 50 mg/L U(VI)/Th(IV) and C_4mimCl in 3 M HNO_3), (c) NTf_2^- concentration (Et-Tol-BPDA), (d) NTf_2^- concentration (Et-Tol-BPymDA) (aqueous phase: 50 mg/L U(VI)/Th(IV) and LiNTf_2 in 3 M HNO_3), (e) NO_3^- concentration (Et-Tol-BPDA), and (f) NO_3^- concentration (Et-Tol-BPymDA) (aqueous phase: 50 mg/L U(VI)/Th(IV) and $\text{Al}(\text{NO}_3)_3$ in 3 M HNO_3) in the aqueous phase. The organic phase was the solutions of 0.5 mM Et-Tol-BPDA or 5 mM Et-Tol-BPymDA in $\text{C}_4\text{mimNTf}_2$.

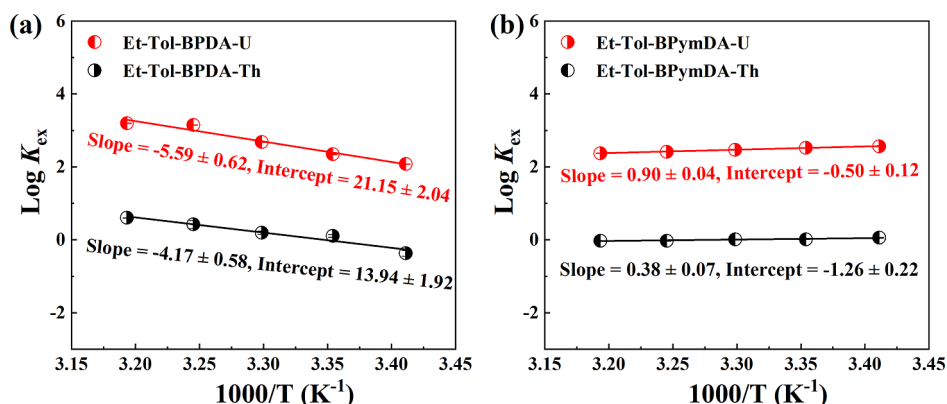


Figure 5. Apparent extraction equilibrium constants $\log K_{\text{ex}}$ of (a) Et-Tol-BPDA or (b) Et-Tol-BPymDA as a function of temperature. Organic phase: 1 mM Et-Tol-BPDA or 5 mM Et-Tol-BPymDA in $\text{C}_4\text{mimNTf}_2$; aqueous phase: 50 mg/L U(VI) or Th(IV) in 3 M HNO_3 .

demonstrate that the extraction reaction is enthalpically driven but entropically disfavored.

UV–Vis Titration Analysis. Solvent extraction studies have shown the high selectivity of Et-Tol-BPDA and Et-Tol-BPymDA for U(VI) over Th(IV). It was, therefore, of significance to compare the complexation behavior and the coordination mode of U(VI) and Th(IV) to rationalize the selectivity. UV–vis spectroscopic experiments were then conducted in acetonitrile at 298 K. As depicted in Figure S12, the results of Job plot experiments indicate the 1:1 stoichiometry between the two ligands and $\text{UO}_2(\text{NO}_3)_2$ or $\text{Th}(\text{NO}_3)_4$ in acetonitrile, which is in good agreement with the

results of slope analyses. A quantitative evaluation of the complexation ability between the two ligands and metal ions was performed by titration of the ligand solution with metal ions. In the case of Et-Tol-BPDA (Figure 6a,b), with the increase of U(VI) or Th(IV) concentration, the absorbance band of Et-Tol-BPDA at 286 nm gradually decreases, while the new absorbance band emerges at wavelengths of 331 nm or 329 nm and increases during the titration, which results in two obvious isosbestic points and implies the formation of new species in solution. As shown in Figure 6c, the initial absorbance band of Et-Tol-BPymDA in the range of 250–350 nm slightly increases with adding U(VI), representing that

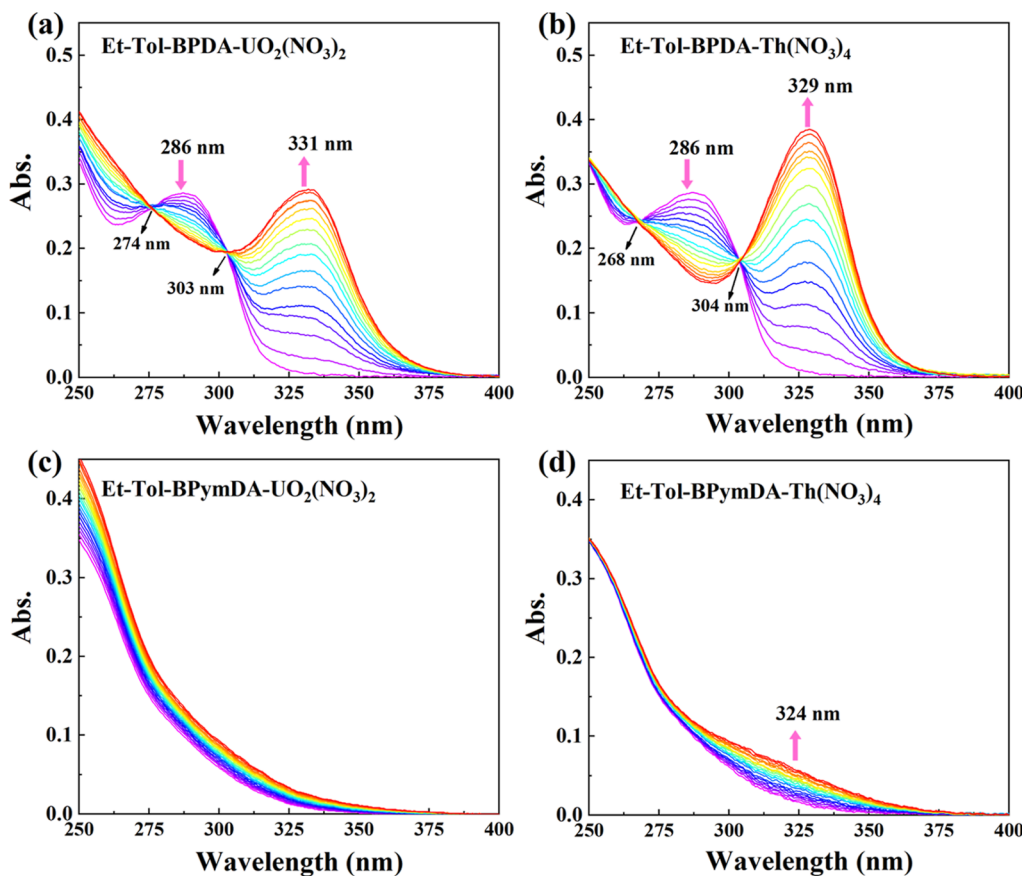


Figure 6. Stacked UV–vis spectra of Et-Tol-BPDA ($20 \mu\text{M}$) titrated with (a) UO_2^{2+} or (b) Th^{4+} in acetonitrile from 0 to 1.5 equiv. Stacked UV–vis spectra of Et-Tol-BPymDA ($20 \mu\text{M}$) titrated with (c) UO_2^{2+} or (d) Th^{4+} in acetonitrile from 0 to 2.0 equiv.

Table 2. Stability Constants ($\log \beta$) for Complexation of U(VI) and Th(IV) with Ligands in Acetonitrile at 298 K

ligand	metal ion	reaction	$\log \beta$	ionic medium
Et-Tol-BPDA	UO_2^{2+}	$\text{L} + \text{UO}_2^{2+} = \text{L}\cdot\text{UO}_2^{2+}$	5.83 ± 0.02	2.5 mM Et_4NNO_3
	Th^{4+}	$\text{L} + \text{Th}^{4+} = \text{L}\cdot\text{Th}^{4+}$	5.08 ± 0.01	2.5 mM Et_4NNO_3
Et-Tol-BPymDA	UO_2^{2+}	$\text{L} + \text{UO}_2^{2+} = \text{L}\cdot\text{UO}_2^{2+}$	3.94 ± 0.01	2.5 mM Et_4NNO_3
	Th^{4+}	$\text{L} + \text{Th}^{4+} = \text{L}\cdot\text{Th}^{4+}$	3.80 ± 0.01	2.5 mM Et_4NNO_3

Et-Tol-BPymDA complexed with U(VI) in acetonitrile. In addition, with the titration of Th(IV), a new absorbance band appears at about 324 nm (Figure 6d), pointing to the complexation of Et-Tol-BPymDA and Th(IV). The stability constant ($\log \beta$) of the 1:1 complex of Et-Tol-BPDA with U(VI) was determined to be 5.83 ± 0.02 by fitting these experimental data (Figures S13–S16). This is greater than that with Th(IV) (5.08 ± 0.01) (Table 2). Similarly, a slightly larger $\log \beta$ value (3.94 ± 0.01) was also found for the complex of Et-Tol-BPymDA with U(VI) compared to that with Th(IV) (3.80 ± 0.01), revealing the stronger binding affinity of the ligands Et-Tol-BPDA and Et-Tol-BPymDA toward U(VI) over Th(IV). This is consistent with the high U(VI)/Th(IV) selectivity observed in solvent extraction experiments. It is apparent that the stability constants of the U(VI)/Th(IV) complexes with Et-Tol-BPDA are much larger than those with Et-Tol-BPymDA. These results demonstrate that the bipyridine-derived amide Et-Tol-BPDA holds a higher affinity toward metal ions with respect to Et-Tol-BPymDA possessing two additional electron-withdrawing nitrogen atoms.

X-ray Crystallographic Structure of U(VI) and Th(IV) Complexes.

To gain more microscopic coordination

information between the two ligands and U(VI) or Th(IV), single crystals of 1:1 complexes of Et-Tol-BPDA or Et-Tol-BPymDA with $\text{UO}_2(\text{NO}_3)_2$ and $\text{Th}(\text{NO}_3)_4$ suitable for crystallographic analysis were successfully obtained by the solvent evaporation method and solvent diffusion method.

The uranyl complexes with Et-Tol-BPDA 3 and Et-Tol-BPymDA 4 are crystallized in the triclinic space group $P-1$ and monoclinic space group $P2_1/c$, respectively. The detailed bond distance and bond angle data are given in Tables S13–S16. In the uranyl complexes 3 and 4 (Figure 7a,c), the uranium center is surrounded by six oxygen atoms and two nitrogen atoms in a weakly distorted hexagonal-bipyramidal coordination mode (Figures 7b,d). Apart from the two axial oxygen atoms, there are two oxygen atoms from a bidentate nitrate anion in the hexagonal equatorial plane, together with two amide oxygen atoms and two pyridine nitrogen atoms or two pyrimidine nitrogen atoms from the ligands (Figures 7a,c). As summarized in Table 3, the average $\text{U}-\text{O}_\text{L}$ bond distance of 2.426 \AA in complex 3 is longer than the corresponding bond distance in complex 4 (2.381 \AA) and the bond distance in the reported uranyl nitrate complex with Et-Tol-DAPhen (2.405 \AA)²² or 4,7-dichloro-1,10-phenanthroline-2,9-(bis-pyrrolidinyl)-

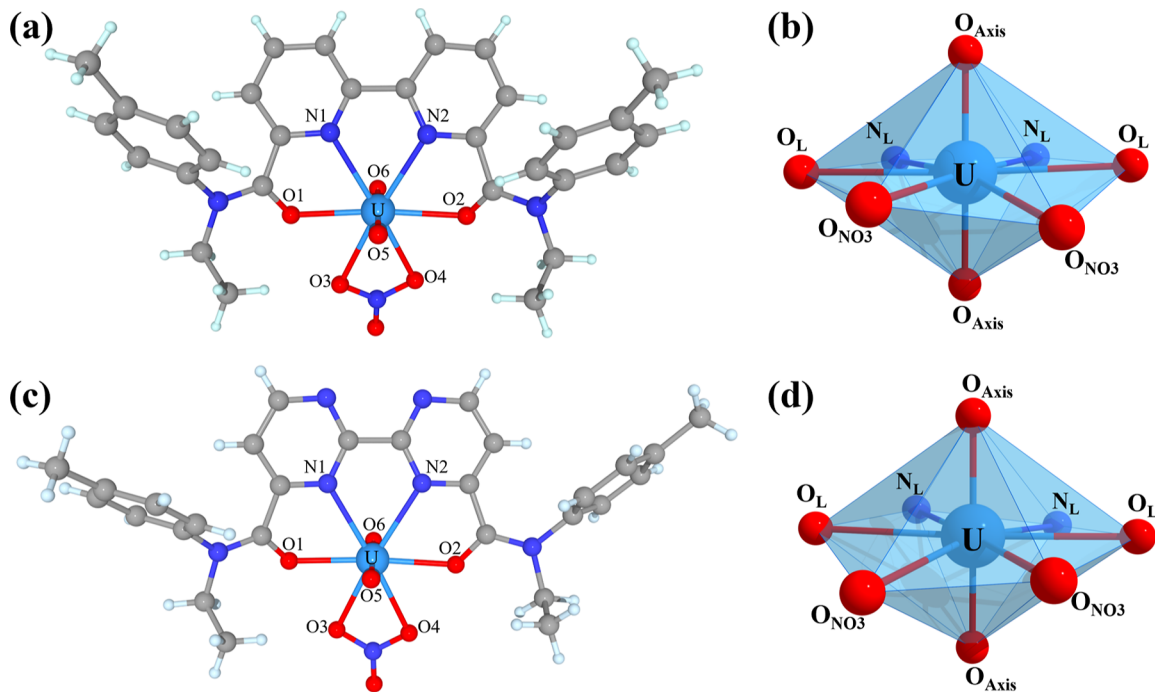


Figure 7. Crystal structures of uranyl complexes with (a) Et-Tol-BPDA 3 and (c) Et-Tol-BPymDA 4. Coordination environment of U(VI) in complexes (b) 3 and (d) 4. The anion in complexes 3 and 4 have been omitted for clarity. Sky blue, gray, blue, red, and light turquoise colors denote U, C, N, O, and H atoms, respectively.

Table 3. Average Bond Distances (Å) Associated with the Central Metal Ion in Complexes 3, 4, 5, and 6

complex	metal ion	average M–N _L	average M–O _L	average M–O _{NO₃}
3	uranyl	2.603(23)	2.426(26)	2.495(27)
4		2.608(25)	2.381(5)	2.512(1)
5	thorium	2.676(2)	2.459(2)	2.591(10)
6		2.684(4)	2.453(3)	2.590(23)

dicarboxamide (2.395 Å).⁴⁸ However, the average bond distance of U–N_L (2.603 Å) in complex 3 is shorter than that in complex 4 (2.608 Å), which indicates that the stronger complexation ability of Et-Tol-BPDA than Et-Tol-BPymDA toward actinides is probably attributable to the stronger M–N_L bonding. This is also corroborated by the longer average Th–O_L bond distance of 2.459 Å in complex 5 (thorium complexed with Et-Tol-BPDA) than that of 2.453 Å in complex 6 (thorium complexed with Et-Tol-BPymDA), and the shorter average Th–N_L bond distance in complex 5 (2.676 Å) than that in complex 6 (2.684 Å). Noteworthily, the average bond distances of U–O_L in uranyl complexes 3 (2.426 Å) and 4 (2.381 Å) are significantly shorter than their corresponding average U–N_L bond distances (2.603 Å and 2.608 Å). A similar trend can also be observed in thorium complexes 5 and 6 and other actinide complexes with N,O-hybrid ligands,^{22,49} which is presumably due to the law that the basicity of the oxygen donor is “harder” than that of the nitrogen donor, resulting in stronger U–O_L bonds in comparison with U–N_L bonds, as uranyl can be recognized as a hard acid.^{14,50}

Figure 8a,c shows the crystal structures of the thorium complexes with Et-Tol-BPDA 5 and Et-Tol-BPymDA 6, which are crystallized in the monoclinic space group I2/a and monoclinic space group C2/c, respectively. The detailed bond distance and bond angle data are given in Tables S17–S20.

The monometallic structure with 1:1 metal-to-ligand stoichiometry for complexes 5 and 6 is in good accord with the results obtained from slope analysis and UV-vis titration experiments. In complexes 5 and 6, the central thorium cation is 12-coordinated with one ligand molecule in a tetradentate fashion through two nitrogen atoms of the bipyridine or bipyrimidine core and two amide oxygen atoms, as well as four bidentate nitrate counterions via oxygen atoms, with the average Th–O_{NO₃} bond distances of 2.591 and 2.590 Å. The resulting thorium coordination polyhedrons can be best described as having a distorted icosahedron geometry (Figures 8b,d), which is also observed in documented thorium-based complexes.^{51,52} Meanwhile, the bond angles of O1–Th–O1 in complexes 5 and 6 are 179.95 ° and 178.29 °, respectively. Figure S17 displays that, unlike the two tolyl groups in the uranyl complexes 3 and 4 on the same side of the bipyridine and bipyrimidine planes, respectively, the two tolyl groups in the thorium complexes 5 and 6 are on the two sides of the bipyridine and bipyrimidine planes, respectively, which might be ascribed to the fact that thorium coordinated with four nitrate ions renders the space too crowded to accommodate two tolyl groups on the same side.²²

CONCLUSIONS

In this work, two new tetradentate N,O-hybrid ligands, Et-Tol-BPDA and Et-Tol-BPymDA, were synthesized for highly selective complexation and extraction of U(VI) over Th(IV) at high acidity. Using C₄mimNTf₂ as the diluent, the SF_{U/Th} values for Et-Tol-BPDA and Et-Tol-BPymDA can achieve as high as 33 and 73, respectively, at 3 M HNO₃. Slope analyses indicated that both U(VI) and Th(IV) are extracted as 1:1 complexes with the two ligands following the solvation mechanism. The 1:1 complexation behaviors of metal ions and ligands were also observed in Job plot experiments carried

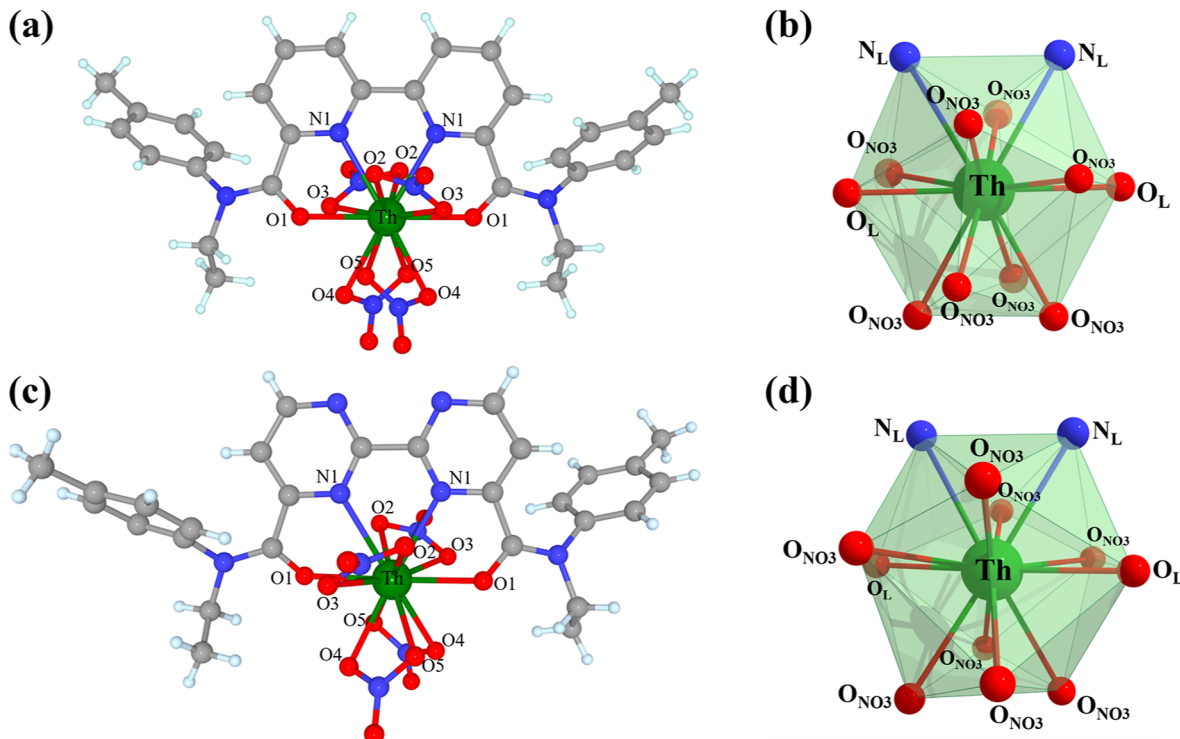


Figure 8. Crystal structures of thorium complexes with (a) Et-Tol-BPDA **5** and (c) Et-Tol-BPyMDA **6**. Coordination environment of Th(IV) in complexes (b) **5** and (d) **6**. Green, gray, blue, red, and light turquoise colors denote Th, C, N, O, and H atoms, respectively.

out in monophasic organic solutions. Evaluation of thermodynamics revealed that the extraction of U(VI) and Th(IV) with the two extractants is spontaneous at room temperature. The stability constants obtained from UV-vis titration experiments proved that Et-Tol-BPDA and Et-Tol-BPyMDA show higher binding affinities toward uranyl ions over thorium ions. The crystal structures disclosed that the uranyl ion is bonded to one Et-Tol-BPDA or Et-Tol-BPyMDA molecule and one bidentate nitrate anion in a near-planar conformation, while the thorium ion is bonded to ligands in a spherical manner with the participation of four nitrate anions. This work provides two promising ligands for U(VI)/Th(IV) separation in highly acidic solutions and enriches our understanding of the coordination chemistry of actinides with N,O-hybrid ligands.

ASSOCIATED CONTENT

Supporting Information

The Supporting Information is available free of charge at <https://pubs.acs.org/doi/10.1021/acs.inorgchem.2c04384>.

Synthetic procedures and characterization spectra; additional extraction experimental results; UV-vis spectrophotometric titration data; and X-ray crystallographic data for ligands Et-Tol-BPDA and Et-Tol-BPyMDA and their complexes with uranyl or thorium (PDF)

Accession Codes

CCDC 2182552–2182554, 2225636–2225637, and 2244159 contain the supplementary crystallographic data for this paper. These data can be obtained free of charge via www.ccdc.cam.ac.uk/data_request/cif, or by emailing data_request@ccdc.cam.ac.uk, or by contacting The Cambridge Crystallographic Data Centre, 12 Union Road, Cambridge CB2 1EZ, UK; fax: +44 1223 336033.

AUTHOR INFORMATION

Corresponding Authors

Yimin Cai – Key Laboratory of Radiation Physics and Technology of the Ministry of Education, Institute of Nuclear Science and Technology, College of Chemistry, Sichuan University, Chengdu 610064, China; Email: ymcai@scu.edu.cn

Wen Feng – Key Laboratory of Radiation Physics and Technology of the Ministry of Education, Institute of Nuclear Science and Technology, College of Chemistry, Sichuan University, Chengdu 610064, China; [0000-0002-1590-071X](https://orcid.org/0000-0002-1590-071X); Email: wfeng9510@scu.edu.cn

Authors

Ying Wang – Key Laboratory of Radiation Physics and Technology of the Ministry of Education, Institute of Nuclear Science and Technology, College of Chemistry, Sichuan University, Chengdu 610064, China

Yuxiang Yang – Key Laboratory of Radiation Physics and Technology of the Ministry of Education, Institute of Nuclear Science and Technology, College of Chemistry, Sichuan University, Chengdu 610064, China

Yijie Wu – Key Laboratory of Radiation Physics and Technology of the Ministry of Education, Institute of Nuclear Science and Technology, College of Chemistry, Sichuan University, Chengdu 610064, China

Jin Li – Key Laboratory of Radiation Physics and Technology of the Ministry of Education, Institute of Nuclear Science and Technology, College of Chemistry, Sichuan University, Chengdu 610064, China

Bowen Hu – Key Laboratory of Radiation Physics and Technology of the Ministry of Education, Institute of Nuclear Science and Technology, College of Chemistry, Sichuan University, Chengdu 610064, China

Lihua Yuan — Key Laboratory of Radiation Physics and Technology of the Ministry of Education, Institute of Nuclear Science and Technology, College of Chemistry, Sichuan University, Chengdu 610064, China; orcid.org/0000-0003-0578-4214

Complete contact information is available at:
<https://pubs.acs.org/10.1021/acs.inorgchem.2c04384>

Notes

The authors declare no competing financial interest.

ACKNOWLEDGMENTS

This work was supported by the National Natural Science Foundation of China (21876121 and 22206138), the Natural Science Foundation of Sichuan Province (2022NSFSC1194), the China Postdoctoral Science Foundation (2022M712229), the Fundamental Research Funds for the Central Universities (2022SCU12123), the Sichuan University Postdoctoral Interdisciplinary Innovation Fund, the Foundation of Key Laboratory of Radiation Physics and Technology of the Ministry of Education (2021SCURPT04), and the Open Project of State Key Laboratory of Supramolecular Structure and Materials (SKLSSM2023032). Analytical & Testing Center of Sichuan University is acknowledged for NMR analysis (Dr. Deng).

REFERENCES

- (1) Abram, T.; Ion, S. Generation-IV nuclear power: A review of the state of the science. *Energy Pol.* **2008**, *36*, 4323–4330.
- (2) Yang, P.; Lin, Z.; Wan, W.; Yu, X.; Cai, X.; Dai, Z.; Dai, Y. The conceptual design of thorium-based molten salt energy amplifier. *Int. J. Energy Res.* **2021**, *45*, 12059–12070.
- (3) David, S.; Huffer, E.; Nifenecker, H. Revisiting the thorium-uranium nuclear fuel cycle. *EuroPhys. News* **2007**, *38*, 24–27.
- (4) Mukerjee, S. K.; Kutty, T. R. G.; Kumar, N.; Pai, R. V.; Kumar, A. Fabrication Technologies for ThO₂-based Fuel. In *Thorium-based Nuclear Fuels. Green Energy and Technology.*; *Green Energy and Technology*; Springer, 2013; pp 205–277.10.1007/978-1-4471-5589-8_6.
- (5) NEA/IAEA, *Uranium 2016: Resources, Production and Demand*, OECD Publishing, Paris, 2016. DOI: 10.1787/uranium-2016-en
- (6) Ünak, T. What is the potential use of thorium in the future energy production technology? *Prog. Nucl. Energy* **2000**, *37*, 137–144.
- (7) Li, R.; Liu, C.; Zhao, H.; He, S.; Li, Z.; Li, Q.; Zhang, L. Di-1-methyl heptyl methylphosphonate (DMHMP): a promising extractant in Th-based fuel reprocessing. *Sep. Purif. Technol.* **2017**, *173*, 105–112.
- (8) Manchanda, V. K.; Pathak, P. N. Amides and diamides as promising extractants in the back end of the nuclear fuel cycle: an overview. *Sep. Purif. Technol.* **2004**, *35*, 85–103.
- (9) Kang, J.; Wu, R.; Li, L.; Hu, H.; Fan, Y.; Jin, Y.; Huang, C.; Chen, J.; Xu, C.; Xia, C. Selective Extraction and Complexation Studies for Thorium(IV) with Bis-triamide Extractants: Synthesis, Solvent Extraction, EXAFS, and DFT. *Inorg. Chem.* **2021**, *60*, 14212–14220.
- (10) Xiong, J.; Hu, S.; Liu, Y.; Yu, J.; Yu, H.; Xie, L.; Wen, J.; Wang, X. Polypropylene Modified with Amidoxime/Carboxyl Groups in Separating Uranium(VI) from Thorium(IV) in Aqueous Solutions. *ACS Sustainable Chem. Eng.* **2017**, *5*, 1924–1930.
- (11) Zhu, Z.; Pranolo, Y.; Cheng, C. Y. Separation of uranium and thorium from rare earths for rare earth production - A review. *Miner. Eng.* **2015**, *77*, 185–196.
- (12) Ang, K. L.; Li, D.; Nikoloski, A. N. The effectiveness of ion exchange resins in separating uranium and thorium from rare earth elements in acidic aqueous sulfate media. Part 1. Anionic and cationic resins. *Hydrometallurgy* **2017**, *174*, 147–155.
- (13) Panak, P. J.; Geist, A. Complexation and Extraction of Trivalent Actinides and Lanthanides by Triazinylpyridine N-donor Ligands. *Chem. Rev.* **2013**, *113*, 1199–1236.
- (14) Chen, L.; Cai, Y.; Feng, W.; Yuan, L. Pillararenes as macrocyclic hosts: a rising star in metal ion separation. *Chem. Commun.* **2019**, *55*, 7883–7898.
- (15) Chandrasekar, A.; Suresh, A.; Joshi, M.; Sundararajan, M.; Ghanty, T. K.; Sivaraman, N. Highly selective separations of U(VI) from a Th(IV) matrix by branched butyl phosphates: Insights from solvent extraction, chromatography and quantum chemical calculations. *Sep. Purif. Technol.* **2019**, *210*, 182–194.
- (16) Leoncini, A.; Huskens, J.; Verboom, W. Ligands for f-element extraction used in the nuclear fuel cycle. *Chem. Soc. Rev.* **2017**, *46*, 7229–7273.
- (17) Biswas, S.; Pathak, P. N.; Singh, D. K.; Roy, S. B. Comparative evaluation of tri-n-butyl phosphate (TBP) and tris(2-ethylhexyl) phosphate (TEHP) for the recovery of uranium from monazite leach solution. *Sep. Sci. Technol.* **2013**, *48*, 2013–2019.
- (18) Biswas, S.; Rupawate, V. H.; Hareendran, K. N.; Roy, S. B. Counter-current extraction and separation of U(VI) from a mixture of U(VI)-Th(IV)-Y(III) using tris-2-ethyl hexyl phosphate (TEHP). *J. Radioanal. Nucl. Chem.* **2013**, *295*, 2243–2248.
- (19) Tan, M.; Huang, C.; Ding, S.; Li, F.; Li, Q.; Zhang, L.; Liu, C.; Li, S. Highly efficient extraction separation of uranium(VI) and thorium(IV) from nitric acid solution with di(1-methyl-heptyl) methyl phosphonate. *Sep. Purif. Technol.* **2015**, *146*, 192–198.
- (20) Verma, P. K.; Pathak, P. N.; Kumari, N.; Sadhu, B.; Sundararajan, M.; Aswal, V. K.; Mohapatra, P. K. Effect of Successive Alkylation of N,N-dialkyl Amides on the Complexation Behavior of Uranium and Thorium: Solvent Extraction, Small Angle Neutron Scattering, and Computational Studies. *J. Phys. Chem. B* **2014**, *118*, 14388–14396.
- (21) Pathak, P. N.; Prabhu, D. R.; Ruikar, P. B.; Mancha, V. K. Evaluation of di(2-ethylhexyl)isobutyramide (D2EHIBA) as a process extractant for the recovery of ²³³U from irradiated Th. *Solvent Extr. Ion Exch.* **2002**, *20*, 293–311.
- (22) Xiao, C. L.; Wang, C. Z.; Yuan, L. Y.; Li, B.; He, H.; Wang, S.; Zhao, Y. L.; Chai, Z. F.; Shi, W. Q. Excellent Selectivity for Actinides with a Tetradentate 2,9-Diamide-1,10-Phenanthroline Ligand in Highly Acidic Solution: A Hard-Soft Donor Combined Strategy. *Inorg. Chem.* **2014**, *53*, 1712–1720.
- (23) Zhang, X.; Yuan, L.; Chai, Z.; Shi, W. A new solvent system containing N,N'-diethyl-N,N'-ditolyl-2,9-diamide-1,10-phenanthroline in 1-(trifluoromethyl)-3-nitrobenzene for highly selective UO₂²⁺ extraction. *Sep. Purif. Technol.* **2016**, *168*, 232–237.
- (24) Matveev, P. I.; Huang, P. W.; Kirsanova, A. A.; Ananyev, I. V.; Sumyanova, T. B.; Kharcheva, A. V.; Khvorostinin, E. Y.; Petrov, V. G.; Shi, W. Q.; Kalmykov, S. N.; Borisova, N. E. Way to Enforce Selectivity via Steric Hindrance: Improvement of Am(III)/Eu(III) Solvent Extraction by Loaded Diposphonic Acid Esters. *Inorg. Chem.* **2021**, *60*, 14563–14581.
- (25) Wang, S.; Wang, C.; Yang, X. F.; Yu, J. P.; Tao, W. Q.; Yang, S. L.; Ren, P.; Yuan, L. Y.; Chai, Z. F.; Shi, W. Q. Selective Separation of Am(III)/Eu(III) by the QL-DAPhen Ligand under High Acidity: Extraction, Spectroscopy, and Theoretical Calculations. *Inorg. Chem.* **2021**, *60*, 19110–19119.
- (26) Xu, L.; Pu, N.; Li, Y.; Wei, P.; Sun, T.; Xiao, C.; Chen, J.; Xu, C. Selective Separation and Complexation of Trivalent Actinide and Lanthanide by a Tetradentate Soft-Hard Donor Ligand: Solvent Extraction, Spectroscopy, and DFT Calculations. *Inorg. Chem.* **2019**, *58*, 4420–4430.
- (27) Meng, R.; Xu, L.; Yang, X.; Sun, M.; Xu, C.; Borisova, N. E.; Zhang, X.; Lei, L.; Xiao, C. Influence of a N-Heterocyclic Core on the Binding Capability of N,O-Hybrid Diamide Ligands toward Trivalent Lanthanides and Actinides. *Inorg. Chem.* **2021**, *60*, 8754–8764.
- (28) Alyapyshev, M. Y.; Babain, V. A.; Tkachenko, L. I.; Paulenova, A.; Popova, A. A.; Borisova, N. E. New Diamides of 2,2'-dipyridyl-6,6'-dicarboxylic Acid for Actinide-Lanthanide Separation. *Solvent Extr. Ion Exch.* **2014**, *32*, 138–152.

- (29) Alyapshev, M.; Babain, V.; Borisova, N.; Eliseev, I.; Kirsanov, D.; Kostin, A.; Legin, A.; Reshetova, M.; Smirnova, Z. 2,2'-Dipyridyl-6,6'-dicarboxylic acid diamides: Synthesis, complexation and extraction properties. *Polyhedron* **2010**, *29*, 1998–2005.
- (30) Zabierowski, P. W.; Jeannin, O.; Fix, T.; Guillemoles, J. F.; Charbonnière, L. J.; Nonat, A. M. From Mono- to Polynuclear Coordination Complexes with a 2,2'-Bipyrimidine-4,4'-dicarboxylate Ligand. *Inorg. Chem.* **2021**, *60*, 8304–8314.
- (31) Alyapshev, M.; Babain, V.; Kirsanov, D. Isolation and Purification of Actinides Using N,O-Hybrid Donor Ligands for Closing the Nuclear Fuel Cycle. *Energies* **2022**, *15*, 7380–7410.
- (32) Zhang, Y. J.; Collison, D.; Livens, F. R.; Powell, A. K.; Wocadlo, S.; Eccles, H. Synthesis, spectroscopic, and X-ray crystallographic characterisation of thorium(IV) and uranium(IV) malonato and substituted malonato compounds. *Polyhedron* **2000**, *19*, 1757–1767.
- (33) Guan, J.; Wang, X.; Shi, P.; Chen, L.; Chen, B.; Zhang, Y.; Chen, Y.; Xu, Y.; Chai, Z.; Wang, S.; Diwu, J. Hinokitiol, an Advanced Bidentate Ligand for Uranyl Decoration. *Inorg. Chem.* **2022**, *61*, 3886–3892.
- (34) Chen, B.; Hong, S.; Dai, X.; Li, X.; Huang, Q.; Sun, T.; Cao, D.; Zhang, H.; Chai, Z.; Diwu, J.; Wang, S. Vivo Uranium Decoration by a Tailor-Made Hexadentate Ligand. *J. Am. Chem. Soc.* **2022**, *144*, 11054–11058.
- (35) Wang, X.; Dai, X.; Shi, C.; Wan, J.; Silver, M. A.; Zhang, L.; Chen, L.; Yi, X.; Chen, B.; Zhang, D.; Yang, K.; Diwu, J.; Wang, J.; Xu, Y.; Zhou, R.; Chai, Z.; Wang, S. A 3,2-Hydroxypyridinone-based Decoration Agent that Removes Uranium from Bones In Vivo. *Nat. Commun.* **2019**, *10*, 2570–2582.
- (36) Zhang, Y.; Bhadbhade, M.; Gao, J.; Karatchevtseva, I.; Price, J. R.; Lumpkin, G. R. Synthesis and crystal structures of uranium(VI) and thorium(IV) complexes with picolinamide and malonamide. *Inorg. Chem. Commun.* **2013**, *37*, 219–221.
- (37) Tutson, C. D.; Gorden, A. E. V. Thorium coordination: A comprehensive review based on coordination number. *Coord. Chem. Rev.* **2017**, *333*, 27–43.
- (38) Lehn, J. M.; De Vains, J. B. R. Synthesis and Properties of Macrocyclic Cryptates Incorporating Five- and Six-Membered Biheteroaryl Units. *Helv. Chim. Acta* **1992**, *75*, 1221–1236.
- (39) Ye, Z. C.; Yang, Z. Y.; Wang, L.; Chen, L. X.; Cai, Y. M.; Deng, P. C.; Feng, W.; Li, X. P.; Yuan, L. H. A Dynamic Hydrogen-Bonded Azo-Macrocycle for Precisely Photo-Controlled Molecular Encapsulation and Release. *Angew. Chem., Int. Ed.* **2019**, *58*, 12519–12523.
- (40) Borisova, N. E.; Ivanov, A. V.; Matveev, P. I.; Smirnova, A. A.; Belova, E. V.; Kalmykov, S. N.; Myasoedov, B. F. Screening of the Structure of Americium Extractants Based on a 2,2'-Bipyridyl Scaffold: a Simple Way to a N₂O₂-Tetridentate Ligands Library for Rational Design of An/Ln Extractants. *ChemistrySelect* **2018**, *3*, 1983–1989.
- (41) Borisova, N. E.; Kostin, A. A.; Eroshkina, E. A.; Reshetova, M. D.; Lyssenko, K. A.; Spodine, E. N.; Puntus, L. N. Lanthanide Complexes with Tetradentate N, N', O, O' -Dipyridyl-Based Ligands: Structure, Stability, and Photophysical Properties. *Eur. J. Inorg. Chem.* **2014**, *2014*, 2219–2229.
- (42) Wu, D.; Cai, P.; Zhao, X.; Kong, Y.; Pan, Y. Recent progress of task-specific ionic liquids in chiral resolution and extraction of biological samples and metal ions. *J. Sep. Sci.* **2018**, *41*, 373–384.
- (43) Mohapatra, P. K. Actinide ion extraction using room temperature ionic liquids: opportunities and challenges for nuclear fuel cycle applications. *Dalton Trans.* **2017**, *46*, 1730–1747.
- (44) Sun, X.; Luo, H.; Dai, S. Ionic liquids-based extraction: a promising strategy for the advanced nuclear fuel cycle. *Chem. Rev.* **2012**, *112*, 2100–2128.
- (45) Billard, I.; Ouadi, A.; Jobin, E.; Champion, J.; Gaillard, C.; Georg, S. Understanding the Extraction Mechanism in Ionic Liquids: UO₂²⁺/HNO₃/TBP/C₄-mimTf₂N as a Case Study. *Solvent Extr. Ion Exch.* **2011**, *29*, 577–601.
- (46) Prabhu, D. R.; Mohapatra, P. K.; Raut, D. R.; Pathak, P.; Billard, I. Extraction of uranium(VI) from nitric acid solutions using N,N-diheptyloctanamide in ionic liquids: Solvent extraction and spectroscopic studies. *Solvent Extr. Ion Exch.* **2017**, *35*, 423–438.
- (47) Chen, L.; Wang, Y.; Yuan, X.; Ren, Y.; Liu, N.; Yuan, L.; Feng, W. Highly selective extraction of uranium from nitric acid medium with phosphine oxide functionalized pillar[5]arenes in room temperature ionic liquid. *Sep. Purif. Technol.* **2018**, *192*, 152–159.
- (48) Gutorova, S. V.; Matveev, P. I.; Lemport, P. S.; Trigub, A. L.; Pozdeev, A. S.; Yatsenko, A. V.; Tarasevich, B. N.; Konopkina, E. A.; Khult, E. K.; Roznyatovsky, V. A.; Nelyubina, Y. V.; Isakovskaya, K. L.; Khrustalev, V. N.; Petrov, V. S.; Aldoshin, A. S.; Ustynyuk, Yu. A.; Petrov, V. G.; Kalmykov, S. N.; Nenajdenko, V. G. Structural Insight into Complexation Ability and Coordination of Uranyl Nitrate by 1,10-Phenanthroline-2,9-diamides. *Inorg. Chem.* **2022**, *61*, 384–398.
- (49) Yang, X. F.; Li, F. F.; Ren, P.; Yuan, L. Y.; Liu, K.; Geng, J. S.; Tang, H. B.; Chai, Z. F.; Shi, W. Q. Selective separation between UO₂²⁺ and Pu⁴⁺ by novel tetridentate chelate phenanthroline diamide ligand in 1-octanol. *Sep. Purif. Technol.* **2021**, *277*, 119521–119529.
- (50) Kolarik, Z. Complexation and Separation of Lanthanides(III) and Actinides(III) by Heterocyclic N-Donors in Solutions. *Chem. Rev.* **2008**, *108*, 4208–4252.
- (51) Liu, W.; Tan, M.; Yu, K.; Tan, G. Synthesis, characterization and crystal structure of complexes of thorium(IV) nitrate with N,N,N',N'-tetraphenyl-3,6-dioxaoctanediamide. *J. Chem. Soc., Dalton Trans.* **1993**, 3427–3430.
- (52) Zhu, L.; Zhu, X.; Zhang, Y.; Li, B.; Cao, Z.; Zhang, Y. Synthesis of thorium (uranyl) sulfoxide complexes and crystal structure of novel thorium complex containing both 10 and 12 coordinated thorium. *J. Mol. Struct.* **2003**, *657*, 375–380.

□ Recommended by ACS

Complexation of a Nitrilotriacetate-Derived Triamide Ligand with Trivalent Lanthanides: A Thermodynamic and Crystallographic Study

Xueyu Wang, Songdong Ding, et al.

FEBRUARY 23, 2023

INORGANIC CHEMISTRY

READ ▶

Solvation-Anionic Exchange Mechanism of Solvent Extraction: Enhanced U(VI) Uptake by Tetridentate Phenanthroline Ligands

Svetlana V. Gutorova, Valentine G. Nenajdenko, et al.

DECEMBER 21, 2022

INORGANIC CHEMISTRY

READ ▶

Understanding the Coordination Chemistry of Am^{III}/Cm^{III} in the DOTA Cavity: Insights from Energetics and Electronic Structure Theory

Yang Gao, Georg Schreckenbach, et al.

FEBRUARY 06, 2023

INORGANIC CHEMISTRY

READ ▶

Theoretical Insights into the Selectivity of Hydrophilic Sulfonated and Phosphorylated Ligands to Am(III) and Eu(III) Ions

Yao Zou, Wei-Qun Shi, et al.

MARCH 09, 2023

INORGANIC CHEMISTRY

READ ▶